

## Liquid Order at the Interface of KDP Crystals with Water: Evidence for Icelike Layers

M. F. Reedijk,<sup>1</sup> J. Arsic,<sup>1</sup> F. F. A. Hollander,<sup>1</sup> S. A. de Vries,<sup>2</sup> and E. Vlieg<sup>1</sup>

<sup>1</sup>*NSRIM Department of Solid State Chemistry, University of Nijmegen, Toernooiveld 1, 6525 ED Nijmegen, The Netherlands*

<sup>2</sup>*FOM-Institute for Atomic and Molecular Physics, Kruislaan 407, 1098 SJ Amsterdam, The Netherlands*

(Received 9 August 2002; published 10 February 2003)

We present a surface x-ray diffraction study on the KDP-water interface in which the structure of both the crystalline and liquid part of the interface has been measured. We have been able to determine the ordering components in the liquid in both the perpendicular and parallel directions. We find interface-induced ordering in the first four layers of water molecules. The first two layers behave icelike and are strongly bound to the surface. The next two layers are more diffuse and show only minor lateral and perpendicular ordering. Subsequent layers are found to behave similar to a bulk liquid.

DOI: 10.1103/PhysRevLett.90.066103

PACS numbers: 68.08.De, 68.35.Bs, 81.10.Dn

Knowledge of the atomic structure of a solid-liquid interface is important in order to understand the different processes occurring at the interface such as crystal growth, lubrication, wetting, or catalysis [1–4]. Owing to the truncation of a crystal at the surface, the atomic structure can differ from the bulk crystallographic structure. Similarly, the liquid near the interface may differ from a bulk liquid, because it is influenced by the periodic potential of the crystal surface and is expected to show more ordering than in a bulk liquid. In the case of crystal growth, these effects will influence parameters such as the incorporation of impurities, the stability of a surface, the growth speed, and the binding of molecules to the surface.

Various theoretical and numerical studies [5–8] show that a liquid at the interface of a crystal exhibits crystal-induced ordering in the first three to four layers. The ordering is predicted to be strongest in the perpendicular direction (layering). Such layering has indeed been observed in a few experimental studies [9–11]. The weaker lateral component has been observed in monolayer thick Pb and Sn films on Ge(111) [12,13]. The picture that emerges from these investigations is that such a “quasiliquid” monolayer has both liquid and solid character. A comparable mix of solid and liquid behavior has been observed in the adsorption of argon on graphite [14,15]. The only observation of lateral liquid ordering in a thicker film was at the interface of solid Si with a Al-Si alloy, where electron microscopy demonstrated this order qualitatively [16].

In this Letter, we present an investigation of the structure of a solid-liquid interface of a crystal in contact with its growth solution in which the ordering components of the liquid near the interface are quantitatively determined for the first time. We find interface-induced ordering in the first four layers of water molecules. The first two layers behave icelike and are strongly bound to the surface. The next two layers are more diffuse and show only minor lateral and perpendicular ordering. The highly ordered “liquid” at the interface is expected to slow down the incorporation and diffusion of the growth units.

As a model system for a solid-liquid interface in crystal growth, we used the {101} face of KDP (KH<sub>2</sub>PO<sub>4</sub>) crystals in contact with ultrathin water layers. KDP crystals can be grown with high quality and are technologically important [17], e.g., in laser systems for harmonic generation and optoelectrical switching. Grown from aqueous solution, two different faces are observed on the morphology of KDP crystals, the {101} and {100} face. The surface structure of the two faces has been determined previously [18]. The {101} face in contact with a saturated aqueous solution of a few micrometers thickness was found to be potassium terminated.

To investigate the atomic structure of the liquid at the interface, surface x-ray diffraction (SXR) is used. SXR can probe the atomic structure of an interface by measuring diffracted intensities along so-called crystal truncation rods [19]. These rods are tails of diffuse intensity connecting the bulk Bragg peaks in the direction perpendicular to the surface. Their exact shape is determined by the interface atomic structure. A partly ordered liquid at the interface will contribute to the diffraction signal from the substrate with a magnitude that depends on the ordering. If the liquid layer is completely disordered parallel to the interface, it does not contribute to rods with an in-plane momentum transfer, but only to the specular rod. If the liquid layer at the interface is partially ordered owing to the periodic potential of the surface, it contributes most strongly to rods with small in-plane momentum transfer. Thus, the amount of ordering in the liquid can be determined by measuring various rods with different in-plane momentum transfer. Figure 1 shows a schematic drawing of a crystal covered with a partly ordered liquid layer and of the varying contribution of the ordered liquid to the different rods in reciprocal space.

In order to detect the small signal from the liquid structure a strong suppression of the background is necessary. We achieved this by using ultrathin water layers. This has a twofold benefit: (i) It reduces the background scattering from the bulk liquid, and (ii) it makes it possible to use x rays with lower energies which in turn reduces the background scattering from the bulk crystal.

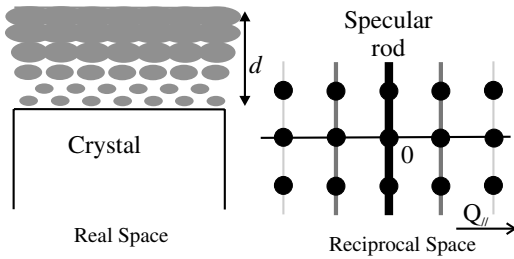


FIG. 1. Schematic drawing of a crystal covered with a partly ordered liquid layer of thickness  $d$ . The contribution of the (partially) ordered liquid to the substrate diffraction rods is strongest in the specular rod and diminishes at higher parallel momentum transfer ( $Q_{\parallel}$ ) in reciprocal space.

AFM and ellipsometry measurements indicate that in a humid environment KDP crystals are covered with an ultrathin water layer [20]. We therefore developed a special temperature controlled “environment cell” in which the relative humidity can be set to 100%. We performed diffraction experiments under several conditions and with different thickness of the water layer. Here we restrict ourselves to the data at 45 °C, where the liquid film was found to be 22 Å thick. By comparing this with the other conditions, we found that this film is infinitely thick for as far as the interface structure is concerned.

The diffraction experiments were performed at beam lines ID3 and ID32 of the ESRF (Grenoble) using a wavelength of  $\sim 1$  Å. The environment cell was mounted on the diffractometer such that the crystal surface normal was in the vertical plane. All data were obtained with a 1.0° incident angle and varying exit angles. We use a surface unit cell for KDP{101} with lattice vectors which are expressed in terms of the conventional tetragonal lattice by  $a_1 = \frac{1}{2}[111]$ ,  $a_2 = \frac{1}{2}[\bar{1}1\bar{1}]$ , and  $a_3 = [\bar{1}01]$  with  $|a_1| = |a_2| = \sqrt{1/2a^2 + 1/4c^2}$  and  $|a_3| = \sqrt{a^2 + c^2}$ , where  $a = 7.45$  Å and  $c = 6.97$  Å are the bulk lattice constants of KDP [21]. The corresponding reciprocal lattice vectors  $\{\mathbf{b}_i\}$  are defined by  $\mathbf{a}_i \cdot \mathbf{b}_j = 2\pi\delta_{ij}$ . The momentum transfer  $\mathbf{Q}$ , which is the difference between the incoming and outgoing wave vectors, can be described by the diffraction indices  $(hkl)$  in reciprocal space:  $\mathbf{Q} = h\mathbf{b}_1 + k\mathbf{b}_2 + l\mathbf{b}_3$ . Here  $h$  and  $k$  are integer values and describe the in-plane part of the momentum transfer, whereas  $l$  is unconstrained and refers to the perpendicular component of the momentum transfer.

We measured an extensive data set, out of which two rods are shown in Fig. 2. All measured intensities were converted into structure factors by applying a standard procedure [22]. Model calculations and fitting were done using the ROD program [23], including the ROBACH extension developed at the ESRF, Grenoble [24]. An indication of the effect of the ordering of the liquid layer on the diffracted intensity can be obtained by comparing the measured structure factors with the ones calculated using the model of De Vries *et al.* (Fig. 2), in which the

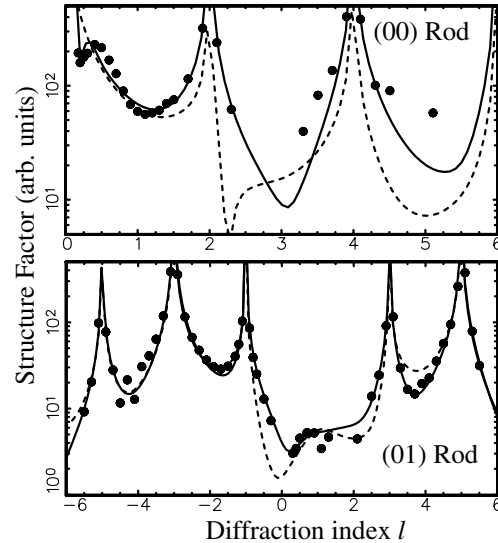


FIG. 2. The data for the  $(hk) = (00)$  and  $(hk) = (10)$  crystal truncation rods, plotted as a function of  $l$ . The solid line is the best fit using the model described in the text. The dashed line is calculated using the model of de Vries *et al.* [18], excluding the water layer.

effects of the liquid were ignored. As expected, large differences are found for the specular rod and smaller differences for the (10) rod, indicating ordering in the water layer.

In order to determine the structure of the liquid, we need a model that describes all features of the interface shown in Fig. 1. Thus, the model must contain a crystalline part describing the KDP crystal surface and a liquid part describing both the ordering properties as well as the thickness of the water layer. A potassium terminated KDP surface, where relaxation of the outermost potassium and phosphate groups is allowed, is used to model the crystalline part. The liquid part of the interface is modeled with planes of oxygen atoms parallel to the surface. Oxygen atoms are used instead of water molecules because x rays are insensitive to hydrogen atoms. By allowing oxygen occupancies larger than 1, we can correct for the fact that the water is probably saturated with the more strongly scattering KDP. The oxygen distribution and periodicity within one layer follow the crystallographic lattice of the KDP surface, each layer consisting of one oxygen atom per unit cell. The strength of the ordering of each layer is fitted through anisotropic Debye-Waller parameters for the oxygen atoms. A small in-plane Debye-Waller parameter corresponds to a layer with high lateral ordering that will contribute to all rods. Bulk liquid layers that contribute only to the specular rod are modeled by giving these a large in-plane Debye-Waller parameter ( $> 1000$ ). We find that the model describes the data well (goodness of fit  $\chi^2$  value of 2.1), including the Kiessig fringe near  $l = 0.4$  of the (00) rod that shows that the total liquid film thickness is 22 Å. Table I lists the

TABLE I. Best fit parameters. All positions ( $x, y, z$ ) are expressed as fractions of the unit cell parameters. Values with a \* were fixed. The Debye-Waller (DW) parameters for  $O_1$  and  $O_2$  were found to converge close to the value for bulk ice and were fixed in the final fit in order to reduce the number of parameters. The occupancy of the fifth oxygen layer and higher are coupled to the fourth oxygen layer as indicated.

	$x$	$y$	$z$	$DW_{\parallel}$	$DW_{\perp}$	Occupancy
$O_n$	...	...	$(1.51 + 0.1)n$	1000*	240(60)	$\text{Occ}(O_4) \times \frac{1}{2} \times \text{erfc}[(z - z_{\text{mean}})/\sqrt{2}]$
$O_4$	...	...	1.51(2)	1000*	240(60)	1.1(1)
$O_3$	0.50(5)	0.47(2)	1.48(2)	12(8)	160(30)	0.7 (1)
$O_2$	0.20(5)	0.77(2)	1.44(2)	1.1*	1.1*	1.4(3)
$O_1$	0.88(5)	0.13(2)	1.39(2)	1.1*	1.1*	2.1(1)
$K^+$	0.75*	0.25*	1.26(3)	1.4*	1.4*	0.69 (4)
$H_2PO_4^-$	0.125*	-0.125*	1.13(2)	0.85*	0.85*	0.93 (2)

best-fit parameters and Fig. 2 shows the best-fit model calculation for the (00) and (01) rods. Note that these results are fully consistent with the data (not shown) at the other conditions and that the error bars reflect this. We find small outward relaxations for the topmost K and  $PO_4$  layers of  $0.09 \pm 0.03 \text{ \AA}$  and  $0.02 \pm 0.02 \text{ \AA}$ , respectively. These values fully agree with the values found by De Vries *et al.* [18].

Somewhat surprisingly, we find the first two water layers near the crystal surface to be well ordered. Subsequent oxygen layers rapidly lose their order; the third layer has both lateral and perpendicular order, the fourth layer only perpendicular. Figure 3 shows the interface structure including the two well-ordered water layers. The two atoms are in close contact with the topmost crystal layer, with which the atoms apparently have quite a strong interaction. Our data show that both atoms have a small Debye-Waller parameter with a value close to the bulk value for ice, indicating a more icelike than liquidlike behavior.

The two oxygen atoms occupy different lateral positions in the unit cell (Fig. 3). The oxygen atoms in the first water layer are very close to the extrapolated lattice position of a next potassium layer. This may imply that this layer, in fact, consists of potassium ions and could be an indication of preordering of these ions in the liquid near the KDP surface. To verify this, a fit was made where the first ordered layer of oxygen atoms is replaced with

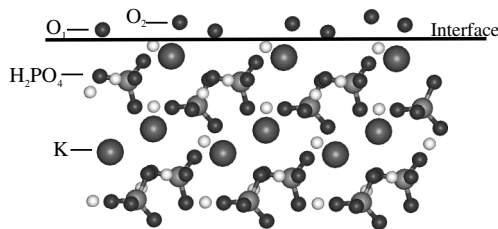


FIG. 3. Schematic side view of the KDP {101} surface, including the two well-ordered water layers represented by O atoms. The first O layer is located close to the extrapolated position of a next K layer.

potassium ions. This results in an equally good fit as in the case of oxygen atoms, but with a reduced occupancy. However, the distance between the two outermost K layers shows an unrealistic 30% compression. It is thus more likely that this layer consists of water molecules that can form hydrogen bonds with the outermost phosphate group (the distance is 3  $\text{\AA}$ ). The oxygen atoms of the second ordered layer are located near the outermost potassium ions and may shield the charge of these ions.

A convenient way to visualize the results is with a projection of the electron density distribution on the  $z$  axis. The in-plane order of the water layer can be taken into account using an additional term in the density distribution depending on the in-plane momentum transfer and in-plane Debye-Waller parameters. Then the density distribution ( $\rho_z$ ) across the interface contributing to a rod with an in-plane momentum transfer  $q_{\parallel}$  can be calculated by a summation over all individual contributions of atoms  $i$  using

$$\rho_z = \sum_i Z_i n_i \exp\left\{-q_{i,\parallel}^2 \frac{DW_{i,\parallel}}{16\pi^2}\right\} \frac{1}{\sigma_{i,\perp} \sqrt{\pi}} \exp\left\{-\frac{(z_i - z)^2}{\sigma_{i,\perp}^2}\right\}, \quad (1)$$

where  $Z$  is the atomic number,  $n$  is the occupancy,  $DW_{\parallel}$  is the in-plane Debye-Waller parameter,  $\sigma_{\perp} = \sqrt{DW_{\perp}/4\pi^2}$  is the mean square vibration amplitude in the out-of-plane direction, and  $z_i$  is the position of atom  $i$ . The first exponential depends on the parallel momentum transfer and shows to which extent the different rods are sensitive to the liquid structure. This factor is 1 for the specular rod, where the parallel momentum transfer is zero and decreases for the other rods depending on the in-plane Debye-Waller factor. In this way, an electron density is obtained depending on the in-plane order of the layer and the momentum transfer. The electron density distribution for the specular rod is the “genuine” distribution, including the diffuse part of the liquid layer. The profile for the other rods shows the part of the electron density that corresponds to this particular Fourier component in the liquid.

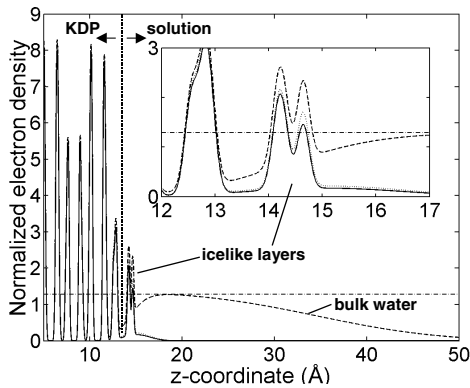


FIG. 4. Electron density distribution across the interface. The electron density is normalized to the electron density of water. The density distribution is shown for three parallel momentum transfers,  $(hk) = (00)$  (dashed line),  $(hk) = (10)$  (dotted line), and  $(hk) = (20)$  (solid line, shown in inset). In addition, the dash-dotted line gives the electron density of a saturated KDP solution. The inset shows an enlargement of the interface area.

Figure 4 shows the electron density profiles across the interface. In all cases, we see the two well-ordered oxygen peaks near the surface. The  $(10)$  and  $(20)$  profiles show in addition a weak contribution from the third water layer. The density for the  $(00)$  rod clearly shows the entire diffuse water layer with a density close to that of a saturated solution, as expected. From the  $(00)$  profile, we find a very gradual liquid/gas interface. Since for our thin layers capillary waves should not play a significant role, this large interface width may be caused by local thickness variations in the film.

The icelike layer at the interface will influence the crystal growth. Growth units can only reach the crystal surface through this layer, and the attachment of the units should therefore be reduced. The activation energy associated with the diffusion through the icelike layer could be one of the rate-limiting factors in the growth [25]. In addition, the surface diffusion of growth units likely occurs on top of the icelike layer, because this will be faster than diffusion at the crystal surface itself. The structure of the icelike layer at a step edge is not known, but the effective liquid order is likely to be less. This would favor incorporation at the step edges with respect to two-dimensional nucleation [26].

On the electrochemical interface of  $\text{RuO}_2(110)$  with water, also icelike layers have been found, but no partly ordered water [27]. Thin water films have been extensively studied in the context of wetting on (biological) materials [3] and evidence for icelike layers was found on mica surfaces [28,29]. Even though mica does not dissolve in water, while in our case the water contains 20 wt % KDP, our x-ray diffraction results lend support for the icelike layers on mica and are in fact a more direct structural determination than the methods used previously [11,29].

In general, our observations agree with earlier theoretical studies that predicted a stronger perpendicular than lateral ordering. The highly ordered first two water layers were unexpected for this crystal in contact with its growth solution. These layers must arise from the strong interactions with the ionic surface, similar to the hydration layers around isolated ions, and deserve further theoretical investigation.

We thank the staff of beam lines ID03 and ID32 of the European Synchrotron Radiation Facility for their valuable assistance during the measurements and J. de Yoreo for providing the KDP crystals. This work is part of the research program of the Foundation for Fundamental Research on Matter (FOM), and was made possible by financial support from the Netherlands Organization for Scientific Research (NWO).

- [1] X.Y. Liu *et al.*, *Nature (London)* **374**, 342 (1995).
- [2] D.W. Oxtoby, *Nature (London)* **347**, 725 (1990).
- [3] J. Hu *et al.*, *Science* **268**, 267 (1995).
- [4] E. Vlieg, *Surf. Sci.* **500**, 458 (2002).
- [5] R.L. Davidchack and B.B. Laird, *J. Chem. Phys.* **108**, 9452 (1998).
- [6] A. Mori, R. Manabe, and K. Nishioka, *Phys. Rev. E* **51**, R3831 (1995).
- [7] F. Spaepen, *Acta Metall.* **23**, 729 (1975).
- [8] A.J.C. Ladd and L.V. Woodcock, *J. Phys. C* **11**, 3565 (1978).
- [9] W.J. Huisman *et al.*, *Nature (London)* **390**, 379 (1997).
- [10] M.F. Toney *et al.*, *Nature (London)* **368**, 444 (1994).
- [11] L. Cheng *et al.*, *Phys. Rev. Lett.* **87**, 156103 (2001).
- [12] F. Grey *et al.*, *Phys. Rev. B* **41**, 9519 (1990).
- [13] M.F. Reedijk *et al.*, *Phys. Rev. B* **64**, 033403 (2001).
- [14] H.S. Youn and G.B. Hess, *Phys. Rev. Lett.* **64**, 918 (1990).
- [15] J.M. Phillips, Q.M. Zhang, and J.Z. Larese, *Phys. Rev. Lett.* **71**, 2971 (1993).
- [16] S. Arai *et al.*, *J. Electron Microsc.* **48**, 317 (1999).
- [17] L.N. Rashkovich, *KDP-Family Single Crystal* (IOP, Bristol, 1991).
- [18] S.A. de Vries *et al.*, *Phys. Rev. Lett.* **80**, 2229 (1998).
- [19] I.K. Robinson, *Phys. Rev. B* **33**, 3830 (1986).
- [20] M.F. Reedijk *et al.* (to be published).
- [21] R. Nelmes, X. Tun, and W. Kuhs, *Ferroelectrics* **71**, 125 (1987).
- [22] E. Vlieg, *J. Appl. Crystallogr.* **30**, 532 (1997).
- [23] E. Vlieg, *J. Appl. Crystallogr.* **33**, 401 (2000).
- [24] O. Robach, [http://www.esrf.fr/computing/scientific/joint\\_projects/ANA-ROD/index.html](http://www.esrf.fr/computing/scientific/joint_projects/ANA-ROD/index.html).
- [25] J.J. DeYoreo, A.K. Burnham, and P.K. Whitman, *Int. Mater. Rev.* **47**, 113 (2002).
- [26] J.J. De Yoreo, T.A. Land, and B. Dair, *Phys. Rev. Lett.* **73**, 838 (1994).
- [27] Y.S. Chu *et al.*, *Phys. Rev. Lett.* **86**, 3364 (2001).
- [28] M. Odelius, M. Bernasoni, and M. Parrinello, *Phys. Rev. Lett.* **78**, 2855 (1997).
- [29] P.B. Miranda *et al.*, *Phys. Rev. Lett.* **81**, 5876 (1998).